

Folic Acid Delivery Device based on Porous Silicon Nanoparticles Synthesized by Electrochemical Etching

Sazan M. Haidary¹, Emma P. Córcoles¹ and Nihad K. Ali^{2,3,*}

¹ Faculty of Biosciences and Medical Engineering,

² Material Innovations and Nanoelectronics Research Group, Faculty of Electrical Engineering,

³ Ibnu Sina Institute for Fundamental Science Studies. Universiti Teknologi Malaysia, 81310 Johor, Skudai, Malaysia

*E-mail: nihad@fke.utm.my

Received: 23 April 2013 / Accepted: 4 June 2013 / Published: 1 July 2013

Folic acid insufficiency has long been related to the occurrence of various diseases. However, the loss of integrity of folic acid has led to the investigation of strategies to improve the vitamin stability and controlled release. Porous silicon nanoparticle is an attractive inorganic material for drug delivery applications due to its biocompatibility and tunable degradation behavior. The aim of this work is to produce porous silicon nanoparticles with suitable dimensions for loading folic acid. Porous silicon was fabricated by anodic electrochemical etching in a Teflon cell containing a 1:4 (v/v) solution of 49% aqueous HF in ethanol. Pores between 15 and 20 nm in diameter were obtained and the highly degradable porous silicon was stabilized to SiO₂ structures by thermal oxidation. Folic acid was loaded into these structures by simple adsorption and the release was examined by UV absorption spectroscopy. The surface morphology of porous silicon delivery device in each stage of the fabrication was characterized by FE-SEM, X-ray spectrometer, FTIR, and XRD and the drug loading confirmed based on the comparison with pure folic acid spectra. pSi nanoparticles showed optimal folic acid delivery capabilities (60 % released after 6 h) and due to its simple fabrication method and its intrinsic optical properties have the potential to be used as a diagnostic and therapeutic point of care tool.

Keywords: Folic acid, Porous silicon, Drug delivery

1. INTRODUCTION

Folic acid is a water-soluble molecule from the B complex of vitamins. The natural occurring form of folic acid, folate, is not synthesized in humans and it is typically obtained through consumption of green vegetables or dietary supplements [1]. Folic acid coenzymes facilitate the

transfer of carbon units, which aid the biosynthesis of purines and pyrimidines, crucial molecules in the synthesis and repair of DNA [2]. Folic acid is known to be essential for the growth and division of cells, which is particularly important during pregnancy and infancy [3]. The insufficiency of folic acid has long been known to be related to certain diseases such as neural tube defects in fetus [4] and megaloblastic anaemia [5]. Other ailments associated with folic acid shortage range from nervous system disturbances [6], for example Alzheimer disease [7], [8], to cardiovascular disorders [9], and cancer [10], [11]. The latter has recently raised controversy, since high levels of folate have been reported to have negative effects in patients with high risk of cancer [12], [13]. On the other hand, the loss of integrity of folic acid, which undergoes degradation when exposed to light, acid or alkaline medium and oxygen atmosphere, has led to the investigation of strategies for improvement of the vitamin stability. Furthermore, since folic acid is easily excreted from the human body, vitamin deficiency usually occurs [14].

The development of materials for the delivery of folic acid either alone or in combination with other drugs for pharmaceutical applications has received great attention. A particular case is the loading of folic acid with anticancer drugs such as doxorubicin [15], [16], [17]. Cancer cells contain greater number of folate receptors compared with normal cells, hence folic acid has been used as a targeting ligand in these anticancer drug delivery systems [18]. Silica modified gold nanorods [19], [20] and folic acid conjugated gold nanoparticles [21] and magnetic nanoparticles [22], [23] have also been investigated for controlled delivery of folic acid.

Since the discovery of its intrinsic visible photo- and electroluminescence properties, nanostructure porous silicon (pSi) has been extensively used in a wide range of applications such as optical and biosensing devices [24], [25]. pSi nanoparticles for drug delivery system can be easily fabricated by electrochemical etching of silicon wafer in an electrochemical solution. The porosity, tunable pore size and the high specific surface area (200–800 m²/g) are responsible for the optical properties of pSi [26]. These characteristics also provide stability in physiological fluids and biocompatibility due to similar silicon levels in blood compared with other physiological elements such as iron, zinc and copper [27]. Furthermore, it degrades into silicic acid, which can be excreted through the urine. This confers silicon its extraordinary biodegradable and non-toxic properties. These characteristics have imparted a significant advantage to pSi compared with other materials, allowing the expansion of pSi to biomedical applications such as radiotherapy [28], tissue engineering [29] and drug delivery devices [30], [31], [32]. pSi nanoparticles are still under investigation. Maniya et al. recently studied the effect of current density and etching time on pore size, porosity, and thickness of the pSi nanoparticles and its application as a carrier for different type of drugs [33].

The development of pSi nanoparticles as drug delivery devices are focused on a particular drug in each case, such as doxorubicin, dexamethasone [34], antipyrine, ibuprofen, griseofulvin, ranitidine and furosemide [35], peptides [36] and anti-cancer drugs such as daunorubicin [37] and mitoxantrone dihydrochloride [38]. To our knowledge folic acid has never been loaded in pSi nanoparticles, but in other types of silicon materials such as silica [39], [15], [17] or together with anticancer drugs [16] and magnetic nanoparticles (Fe₂O₃-SiO₂) [23]. Hence, we aim to investigate the use of pSi nanoparticles as potential folic acid carriers. For this, the fabricated pSi was first characterized by Field Emission Scanning Electron Microscopy (FE-SEM) and the chemical compositions of the samples were

determined by an Energy Dispersive X-ray (EDX) Spectrometer, X-ray diffraction (XRD), (FTIR) Fourier transform infra red spectroscopy. The release of the drug was monitored by UV absorption spectroscopy.

2. MATERIALS AND METHODS

2.1. Chemicals and Solutions

All chemicals, hydrofluoric acid 49%, ethanol alcohol, ammonium hydroxide, hydrochloric acid, hydrogen peroxide and phosphate buffer saline (PBS) were purchased from Sigma Aldrich (Malaysia). The n-type Si wafers (single crystalline n-type, 0.008-0.018 Ω resistivity and <100> orientation) were purchased from Siltronix SAS (Archamps, France).

2.2. Preparation of pSi nanoparticles

Porous silicon samples were prepared from single crystalline n-type Si wafers. These were first cleaned in a solution of 1:1:5 $\text{NH}_4\text{OH}:\text{H}_2\text{O}_2:\text{H}_2\text{O}$ for 10 min at 70-80 °C, then in 1:50 $\text{HF}:\text{H}_2\text{O}$ for 15 sec and finally in 1:1:6 $\text{HCL}:\text{H}_2\text{O}_2:\text{H}_2\text{O}$ for 10 min at 70-80 °C. Porous silicon was fabricated by anodic electrochemical etching in a Teflon cell containing a 1:4 (v/v) solution of 49% aqueous HF in ethanol. The current density was held at 20 mA/cm^2 for 30 min and the sample was illuminated with an incandescent white light of 40 W. Lift-off methods were utilized for removing the porous layer from Si substrate with application of current density of 250 mA/cm^2 for 30 sec, and then porous layer converted into microparticles by using ultrasonic fracture.

Chemical oxidation of pSi films was carried out by thermal oxidation. The pSi nanoparticles were heated at 800 °C in the oven for 1 hour and then the sample was allowed to slowly cool down to room temperature.

2.3. Loading Folic Acid on the pSi Nanoparticles

The folic acid solution consisted of (10 mg/ml) in sodium hydroxide. The particles were soaked in drug solution for 3 hours and this was stirred at intervals to allow homogeneity. After that the solvent was allowed to evaporate. The particles were briefly rinsed with deionized water to remove any excess drug remaining on the surface that had not infiltrated the pores.

2.4. Characterization

Following each of the steps during the fabrication of pSi as a drug carrier (i.e: electrochemical etching, oxidation and loading) the samples were characterized by Field Emission-Scanning Electron Microscopy (FE-SEM) JSM-6701F to observe the surface of porous silicon and Energy Dispersive X-

ray Spectroscopy EDX to provide elemental analysis. Other techniques such as X-ray diffraction (XRD) and FTIR were used to investigate the pSi fabrication, modification and folic acid loading process.

3. RESULTS AND DISCUSSION

3.1. Fabrication of pSi by Electrochemical Etching

In this work we have studied pSi nanoparticles prepared by electrochemical etching as a drug carrier device for loading folic acid. Firstly, we studied the porosity characterized by FE-SEM as shown in (Fig. 1).

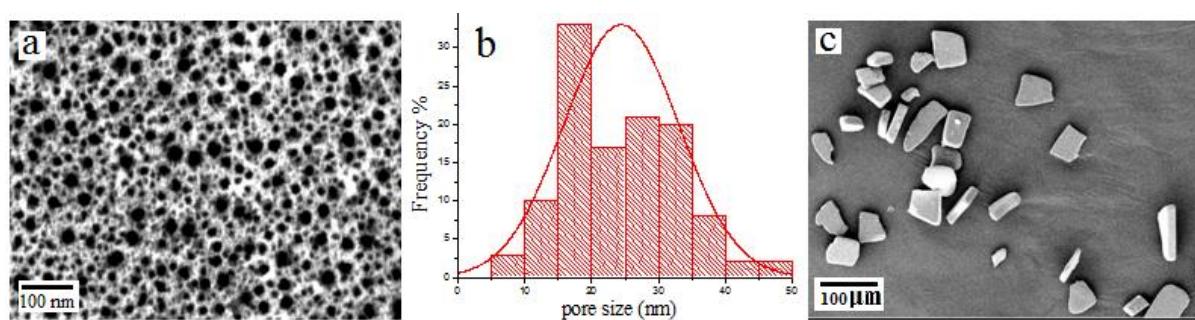


Figure 1. (a) FESEM image of porous silicon (b) pore size distribution histogram (c) FESEM image of porous silicon microparticles after fracturing by sonication.

Fig. 1a shows the FE-SEM image carried out to determine the optimum morphology of the pSi formed. The pores diameter, calculated by ImageJ software, ranged between 5 to 50 nm with an average pore distribution between 15 to 20 nm as shown in the histogram graph (Fig. 1b). The pores appear uniformly distributed throughout the structures suggesting an appropriated fabrication method. Furthermore, the pore size agrees with the optimum pore size for loading low molecular weight drugs [40], [41]. Figure 1c shows the FE-SEM image of Si nanoparticles after fracture by sonication. The image reveals uniform microparticles, with an average size of $40 \pm 5 \mu\text{m}$ and high specific surface area ($460 \text{ m}^2/\text{g}$), calculated with nitrogen gas according to Brunauer–Emmett–Teller (BET) theory [42], which allows the loading of folic acid.

3.2. pSi Surface Modification and Drug Loading Process

Following the fabrication of pSi nanoparticles the surface was modified by thermal oxidation in the oven at $800 \text{ }^\circ\text{C}$ for 60 min. The oxidation process increases the stability of the material in aqueous solvents and decreases the hydrophobicity of silicon [43]. EDX was used to confirm the elemental analysis of the pSi samples at various steps of the fabrication process (Fig. 2). A single peak corresponding to Si was observed in the elemental analysis of fresh pSi (Si wafer after etching) (Fig.

2a). Following thermal modification, oxygen atomic percentages were perceived (Fig. 2b), confirming the incorporation of oxygen on the surface of pSi during the oxidation process. EDX for folic acid was performed as a reference, confirming its chemical structure ($C_{19}H_{19}N_7O_6$) (Fig. 2c). Hence, the existence of carbon and nitrogen atomic percentages in Fig. 2d was attributed to the loading of folic acid into pSi. The elemental analysis of folic acid loaded in oxidized pSi (Fig. 2e) showed a lower loading rate compared with freshly prepared pSi (Fig. 2d), due to the shrinking of the pores during the oxidation process.

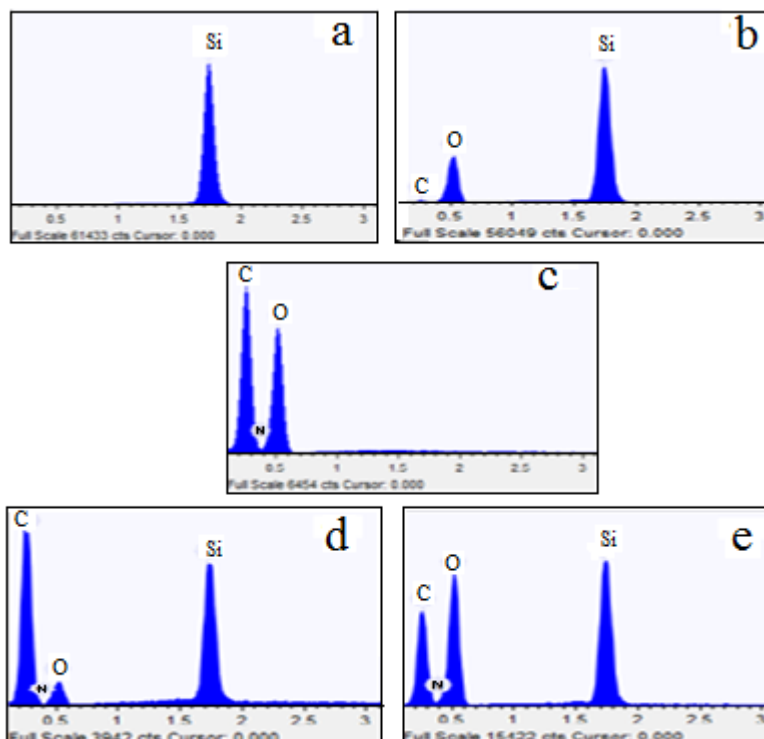


Figure 2. EDX spectrum of a) freshly prepared pSi nanoparticles, b) oxidized pSi nanoparticles, c) pure folic acid, d) folic acid loaded in freshly prepared pSi nanoparticles and e) folic acid loaded in oxidized pSi nanoparticles.

3.3. X-ray diffraction (XRD) Analysis

X-ray diffraction analysis of pSi nanoparticles was performed with a Bruker D8 Advance diffractometer (XRD). Fig. 3 presents the XRD data recorded in the 2θ range ($0-70^\circ$) of pSi nanoparticles, pSi after thermal surface modification and pSi after loading of folic acid. The XRD data of pSi nanoparticle showed a sharp peak at $2\theta = 69^\circ$ corresponding to the (400) plane reflection of Si (Fig. 3a). The XRD pattern of oxidized porous silicon crystal structure is observed in Fig. 3b. During thermal surface modification at 800°C the Si is oxidized to SiO_2 , resulting in a new crystalline structure (SiO_2 crystalline structure, JCPDS 39-1425 [44]) and a reduction of the Si pores size. This reduction of pores size is observed in the reduction of intensity peak in the XRD data [45]. The diffraction peaks of folic acid are reported to be at 2θ between 10° and 30° [46] with a centered peak at

$\sim 22^\circ$ [47]. This folic acid peak at $2\theta \sim 22^\circ$ and the pSi peak at $2\theta \sim 69^\circ$ are observed in the XRD data in Fig 3c confirming the successful loading of folic acid into pSi nanoparticles.

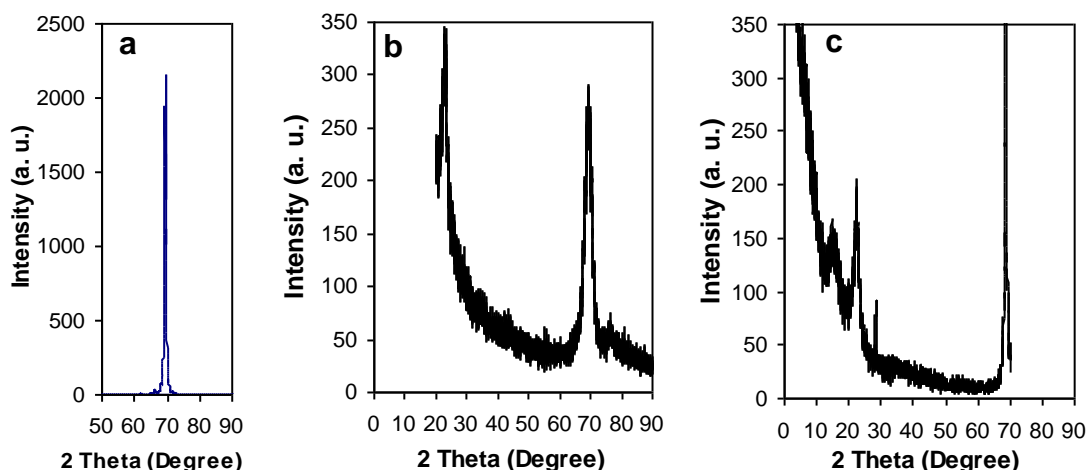


Figure 3. XRD pattern of a) freshly prepared pSi, b) oxidized pSi at 800°C and c) pSi loading with folic acid.

3.4. FTIR Spectroscopy

Fourier transform infrared (FTIR) spectroscopy was used to investigate the chemical bonds of the pSi nanoparticles at different stages of the fabrication procedure over the wave number range $500\text{--}4000\text{ cm}^{-1}$. Before loading the folic acid, the FTIR spectrum of the freshly etched pSi displays bands characteristic of surface hydride species (Fig. 4a). This spectrum shows a number of absorbance bands, the band at 2100 cm^{-1} is attributed to the stretching mode of SiH [34]. The Si-O-Si absorbance observed at 1069 cm^{-1} is due to the oxidation of the sample while handling the preparation pallet for FTIR analysis. The absorbance observed at 621 cm^{-1} and 872 cm^{-1} are attributed to different SiH_x deformation modes [48]. Fig. 4b shows the spectrum after oxidation of pSi at 800°C . Here the Si-O-Si absorbance at 1069 cm^{-1} , due to the oxidation of the sample and new vibrational modes at 3412 cm^{-1} attributed to Si-OH, are observed [49]. Folic acid was loaded into the fabricated pSi nanoparticles following surface modification. The FTIR spectrum of this sample (Fig. 4c) shows absorption at different wave numbers, 1637.01 cm^{-1} for the carbonyl group, 1384.38 cm^{-1} (C=C), 1477 cm^{-1} (phenyl, pterin ring) and 3442.13 cm^{-1} due to hydroxyl stretching bonds and NH group [50]. Folic acid is composed of p-amino benzoic acid, glutamic acid and a hetero-bicyclic pteridine [50] as observed in its FTIR spectrum (Fig. 4d). Hence, the successful loading of folic acid can be confirmed by the comparison of the infrared spectrum of nanoparticles with the infrared spectrum of pure folic acid.

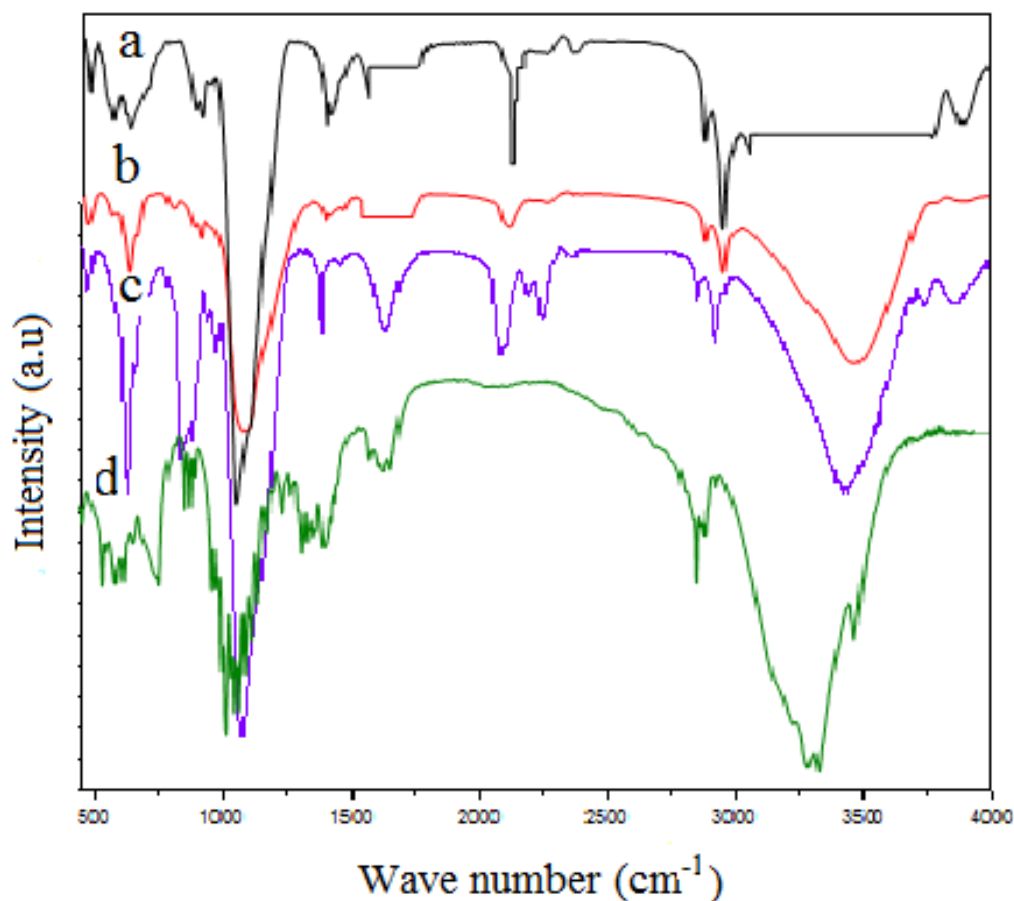


Figure 4. Fourier transform infrared (FTIR) spectra of different pSi nanoparticles, showing a) freshly etched pSi, b) the oxidized pSi nanoparticles treated by thermal oxidation at 800 °C, c) oxidized pSi after drug loading displaying the characteristic vibrational bands of folic acid and d) reference spectrum of folic acid.

3.5. *In vitro* Release

Pharmacological compounds of folic acid are prepared in alkaline media due to its higher stability and solubility. Typically folic acid tablets are administered orally and the active principle is absorbed through the intestinal walls. However, the acidic environment of the stomach degrades the active principle of the drug before this can be absorbed through the intestines [51]. Hence, slightly basic pH media are commonly used to monitor the release of folic acid from the carrier device.

Since the rate of release of the drug is limited by the degradation of the device itself, the release of folic acid from the pSi nanoparticles was monitored as a function of time. UV absorption spectroscopy was used to monitor the drug release at pH 7.4 in PBS solution at intervals of approximately 40 min during 6 h. The solution absorbance band at 300 nm increased with time as the folic acid is released from the oxidized porous silicon nanoparticles as observed in Fig. 5.

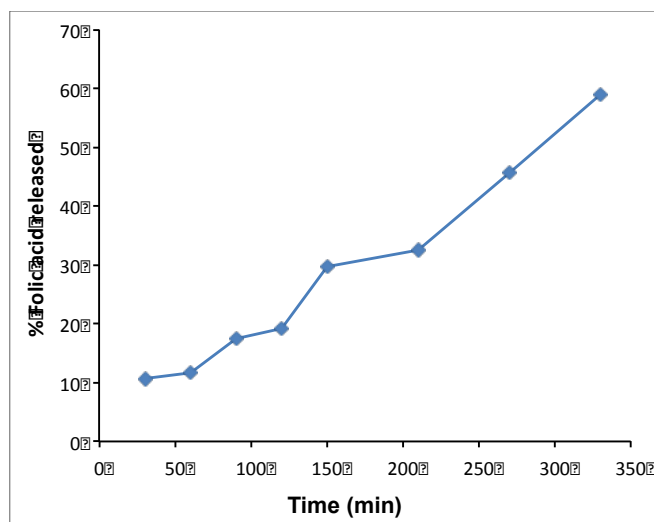


Figure 5. Percentage of folic acid released in PBS as a function of time monitoring by UV absorption spectroscopy (pH = 7.4 and $\lambda = 300$ nm).

Table 1. Percentage of folic acid released in different drug delivery devices.

Devices	Released %	Time	pH of Solution	Publication
Ethyl Cellulose Microcapsules	32% and 70%	1 and 6 h, respectively	pH = 7.4	[52]
Commercial folic acid tablet	60% and 90%	1 and 5 h, respectively	pH = 7.4	[52]
Sodium alginate-pectin-poly(ethylene oxide) electrospun fibers	90-100%	2h	pH = 7.8	[53]
Poly(DL-lactide-co-glycolide) Nanospheres	20 % and > 82%	12 and 30 days, respectively	pH = 7.4	[54]
Polyion complex micelles (PICMs)	60 and 90-100%	2 and 10 h, respectively	pH = 7.4	[55]
Porous silicon nanoparticles	~10 % and ~60 %	1 and 5 ½ h, respectively	pH = 7.4 (PBS)	this work

Results showed that folic acid was released within one hour from immersion in the PBS and continue to increase with time. After 330 min 58.87% of folic acid was released from the stable pSi surface. This presents longer released times compared with the commercial folic acid tablets, which at pH of 7.4 showed a released of 60% and 90% after 1 and 5 h, respectively [52]. Other drug carriers produced for the delivery of folic acid showed a range of percentage released and time depending on the material used (Table 1). These differences may be useful for different applications, where a carrier might be chosen depending on the amount of drug released required. Nevertheless, pSi nanoparticles are relatively simple to fabricate and provide an excellent release rate, which depends on the hydrolysis reaction of pSi with water. Silicon presents a low solubility in water, which counts for its reversibility, however, silicon solubility increases with the pH of the solution as shown in [16].

Anyhow, the solubility of pSi can be further controlled with polymer coatings. In addition pSi presents outstanding optical and biocompatibility properties, allowing the combination of imaging, biosensing and drug delivery capabilities to create 'close-loop' systems for the improvement of diagnostic and therapeutic healthcare.

4. CONCLUSION

The feasibility of pSi as folic acid delivery device was investigated in this study. The device was fabricated by electrochemical etching of silicon wafer, resulting in porous microparticles, which were further stabilized by thermal oxidation. Folic acid was successfully loaded in the nanoporous silicon and confirmed by EDX, XRD and FTIR based on the comparison with pure folic acid. The release of folic acid was monitored by UV absorption spectroscopy showing a 10 % and 60 % release after 30 min and 6 h, respectively. This corresponds with a slower degradation rate compared with commercial folic acid tablets and agrees with other drug delivery materials. Overall, pSi nanoparticles present optimal folic acid delivery capabilities and together with its intrinsic optical properties and biocompatibility have the potential to be used as wearable devices for point of care, where the diagnosis triggers the drug release.

ACKNOWLEDGEMENTS

The authors acknowledge the support of Malaysian Ministry of Higher Education (MOHE) and Universiti Teknologi Malaysia (UTM) through the University Research Grant vote # J.130000.7836.01H78, and 02H83.

References

1. M. Tuszyńska, *Veg. Crops Res. Bull.*, 76 (2012) 43-54.
2. M. Lucock, *Mol Gen Meta*, 71 (2000) 121-138.
3. Y. Lamers, *Ann Nutr Metab*, 59 (2011) 32-37.
4. H. Heseke, *Ann Nutr Metab*, 59 (2011) 41-45.
5. J.M. Scott, and A.M. Molloy, *Ann Nutr Metab*, 61 (2012) 239-245.
6. M. Serrano, B. Pérez-Dueñas, J. Montoya, A. Ormazabal, and R. Artuch, *Drug Discov Today*, 17 (2012) 1299-1306.
7. S. Lopera, C. Guzmán, C. Cataño, and C. Gallardo, *Vitae*, 16 (2009) 55-65.
8. M. Hinterberger, and P. Fischer, *J Neural Transm*, 120 (2013) 211-224.
9. A. Kolb, L. Petrie, *Mol Immunol*, 54 (2013) 164-172.
10. S. Duthie, *BRIT MED BULL*, 55 (1999) 578-592.
11. A. Alshatwi, *FOOD CHEM TOXICOL*, 48 (2010) 1881-1885.
12. J. Kotsopoulos, Y. Kim, and S. Narod, *CANCER CAUSE CONTROL*, 23 (2012) 1405-1420.
13. K. Lubecka-Pietruszewska, A. Kaufman-Szymczyk, B. Stefanska, and K. Fabianowska-Majewska, *Biochem. Biophys. Res. Commun*, 430 (2013) 623-628.
14. Z. Wu, Y. Jiang, T. Kim, and K. Lee, *J. Control. Release*, 119 (2007) 215-221
15. R. Guo, L. Li, W. H. Zhao, Y. X. Chen, X. Z. Wang, C. J. Fang, W. Feng, T. L. Zhang, X. Ma, M. Lu, S. Q. Peng, and C. H. Yan, *Nanoscale*, 4 (2012) 3577-3583.
16. O. Tabasi, C. Falamaki, and Z. Khalaj, *Colloids Surf. B*, 98 (2012) 18-25.

17. F. Gao, L. Li, T. Liu, N. Hao, H. Liu, L. Tan, H. Li, X. Huang, B. Peng, C. Yan, L. Yang, X. Wu, D. Chen, and F. Tang, *Nanoscale*, 4 (2012) 3365-3372.
18. J.M. Rosenholm, A. Meinander, E. Peuhu, R. Niemi, J.E. Eriksson, C. Sahlgren, and M. Lindén, *ACS Nano*, 3 (2009) 197-206.
19. P. Huang, L. Bao, C. Zhang, J. Lin, T. Luo, D. Yang, M. He, Z. Li, G. Gao, B. Gao, S. Fu, and D. Cui, *Biomaterials*, 32 (2011) 9796-9809.
20. H. Wang, L. Zheng, C. Peng, M. Shen, X. Shi, and G. Zhang, *Biomaterials*, 34 (2013) 470-480.
21. Z. Zhang, J. Jia, Y. Ma, J. Weng, Y. Sun, and L. Sun, *MedChemComm*, 2 (2011) 1079-1082.
22. M. Heidari Majd, D. Asgari, J. Barar, H. Valizadeh, V. Kafil, A. Abadpour, E. Moumivand, J. S. Mojarrad, M. R. Rashidi, G. Coukos, and Y. Omid, *Colloids Surf. B*, 106 (2013) 117-125.
23. L. Wang, K.G. Neoh, E.T. Kang, and B. Shuter, *Biomaterials*, 32 (2011) 2166-2173.
24. A.V. Pavlikov, A.V. Lartsev, I.A. Gayduchenko, and V. Yu Timoshenko, *Microelectron. Eng.*, 90 (2012) 96-98.
25. F. Demami, L. Ni, R. Rogel, A.C. Salaun, and L. Pichon, *Procedia Eng.*, 2010, 351-354.
26. J. Salonen, and V.P. Lehto, *Chem. Eng. J.* 137 (2008) 162-172.
27. N.B. Roberts, and P. Williams, *Clinical Chemistry*, 36 (1990) 1460-1465.
28. C. Talamonti, M. Bruzzi, L. Marrazzo, D. Menichelli, M. Scaringella, and M. Bucciolini, *NUCL INSTRUM METH A*, 658 (2011) 84-89.
29. S.D. Alvarez, A.M. Derfus, M.P. Schwartz, S.N. Bhatia, and M.J. Sailor, *Biomaterials*, 30 (2009) 26-34.
30. E.J. Anglin, L. Cheng, W.R. Freeman, and M.J. Sailor, *Adv. Drug Delivery Rev.*, 60 (2008) 1266-1277.
31. D.S. Kumar, D. Banji, B. Madhavi.B, V. Bodanapu, and S. Dondapati, A.P. Sri, *Int J Pharm Pharm Sci*, 2 (2009) 8-16.
32. S.M. Haidary, E.P. Córcoles, and N.K. Ali, *J NANOMATER*, 2012 (2012) 15.
33. N.H. Maniya, S.R. Patel, Z.V.P. Murthy, *SUPERLATTICE MICROST*, 55 (2013) 144-150.
34. E.J. Anglin, M.P. Schwartz, V.P. Ng, L.A. Perelman, and M.J. Sailor, *Langmuir*, 20 (2004) 11264-11269.
35. J. Salonen, L. Laitinen, A.M. Kaukonen, J. Tuura, M. Björkqvist, T. Heikkilä, K. Vähä-Heikkilä, J. Hirvonen, and V.P. Lehto, *J. Control. Release*, 108 (2005) 362-374.
36. M. Kovalainen, J. Mönkäre, M. Kaasalainen, J. Riikonen, V.P. Lehto, J. Salonen, K.H. Herzig, and K. Järvinen, *Mol. Pharm.*, 10 (2013) 353-359.
37. J. Chhablani, A. Nieto, H. Hou, E.C. Wu, W.R. Freeman, M.J. Sailor, and L. Cheng, *Invest Ophthalmol Vis Sci*, 54 (2013) 1268-1279.
38. A. Tzur-Balter, A. Gilert, N. Massad-Ivanir, and E. Segal, *Acta Biomaterialia*, (2013).
39. V. Lebret, L. Raehm, J.O. Durand, M. Smaïhi, M.H.V. Werts, M. Blanchard-Desce, D. Méthy-Gonnod, and C. Dubernet, *J. Biomed.*, 6 (2010) 176-180.
40. A.M. Kaukonen, L. Laitinen, J. Salonen, J. Tuura, T. Heikkilä, T. Linnell, J. Hirvonen, and V.P. Lehto, *EUR J PHARM BIOPHARM*, 66 (2007) 348-356.
41. A. Bragaru, K. Mihaela, M. Simion, A. Iordanescu, R. Pascu, B.M. Danila, F. Craciunoiu, and M. Diaconu, *SIMCND*, 1 (2011) 117-120.
42. J.B. Condon, *Surface Area and Porosity Determinations by Physisorption*, Elsevier 2006.
43. E. Pastor, E. Matveeva, A. Valle-Gallego, F.M. Goycoolea, and M. Garcia-Fuentes, *Colloids Surf. B*, 88 (2011) 601-609.
44. R. Cisneros, H. Pfeiffer, and C. Wang, *NANOSCALE RES LETT*, 5 (2010) 686-691.
45. A.E. Pap, K. Kordás, G. Tóth, J. Levoska, A. Uusimäki, J. Vähäkangas, S. Leppävuori, and T.F. George, *Appl. Phys. Lett.*, 86 (2005) 041501-1-041501-3.
46. A. Vora, A. Riga, D. Dollimore, and K.S. Alexander, *THERMOCHIM ACTA*, 392-393 (2002) 209-220.

47. M.G. Florea, A. Fikai, O. Oprea, C. Guran, D. Fikai, L. Pall, and E. Andronescu, *REV ROM MATER*, 42 (2012) 313-316.
48. P. Gupta, V. Colvin, S. George, *Phys. Rev.*, 37 (1988) 8234.
49. M.A. Vásquez-A, G. Águila Rodríguez, G. García-Salgado, G. Romero-Paredes, and R. Peña-Sierra, *Rev Mex Fis*, 53 (2007) 431-435.
50. Y.Y. He, X.C. Wang, P.K. Jin, B. Zhao, and X. Fan, *SPECTROCHIM ACTA A*, 72 (2009) 876-879.
51. I.R. Younis, M.K. Stamatakis, P.S. Callery, and P.J. Meyer-Stout, *Int. J. Pharm.* 367 (2009) 97-102.
52. S. Prasertmanakit, N. Praphairaksit, W. Chiangthong, and N. Muangsin, *AAPS PharmSciTech*, 10 (2009) 1104-1112.
53. T. Alborzi, K. Lim, Y. Kakuda, *J Microencapsul*, 30 (2013) 64-71.
54. M. Stevanovi, A. Radulovi, B. Jordovi, and D. Uskokovi, *J. Biomed. Nanotechnol.*, 4 (2008) 349-358.
55. Y. Luo, J. Yuan, J. Shi, and Q. Gao, *J. Colloid Interface Sci.*, 350 (2010) 140-147.